Clay Assemblage and Oxygen Isotopic Constraints on the Weathering Response to the PE Thermal Maximum, East Coast of North America"

Appendix DR1

DETAILED GEOLOGICAL SETTING AND METHODS

For our study, we selected ODP Leg 174AX Site "Bass River" (39°36'42''N, 74°26'12''W; Fig. DR1) (Miller et al., 1998), on the New Jersey coastal plains. This site affords several advantages: (1) previous studies documented a regional peak in kaolinite at the PETM (Gibson et al., 2000), (2) a detailed stable isotope stratigraphy (using both bulk-rock and genus-specific foraminifers) has already been established for this site, demonstrating completeness and providing constraints for the age model (John et al., 2008), and (3) biostratigraphic and organic geochemical evidence for other environmental changes including SST and SSS also exist (Sluijs et al., 2007). During the mid to late Paleocene, Bass River was located close to the shelf edge (Miller et al., 2004). Upper Paleocene sediments are characterized by glauconite-rich sand to silts, while sediments just below the Paleocene/Eocene (P/E) boundary that extend into the lower Eocene are more clay-rich (John et al., 2008). The Bass River cores were sampled at the resolution needed to capture the onset of the PETM more precisely: about one sample every 1.5 m between 368.03-359.10 meters below surface (mbs), every 0.2 m between 359.10 and 355.14 mbs, and every 1.2 m between 355.14 and 345.17 mbs.

Clay (<2 μm size-fraction) separations were conducted at the University of California, Santa Cruz, following the settling method based on Stoke's law described in Moore and Reynolds (1997). X-ray diffraction (XRD) analysis of the separated clays was performed in the Laboratory for Stable Isotope Science (LSIS) at the University of West Ontario on 30-40 mg aliquots of crushed, freeze-dried clay sample dispensed in 2mL of distilled water and pipetted onto glass slides. Clay mineralogy was determined by analysis of three XRD aliquots per sample: air-dried, glycolated and baked (550˚C for 2 hours) sub-sample, in that order. Measurements were performed on a Rigaku rotating-anode XRD employing CoKα radiation, with monochromation achieved using a curved crystal, diffracted beam, graphite monochromater, and operated at 45kV and 160mA with a scan rate of 10° 2θper minute (equivalent to 0.5° 2θ on conventional diffractometers). The scanning range was 2 to 42° 2θ for the air-dried and heated trials, and 2 to 82° 2θ for the glycolated trial. The spacing for the first low angle diffraction of clay minerals was examined for each trial and compared to patterns presented by Brindley and Brown (1980) in order to determine the phases present in each sample.

The relative percentages of individual clay minerals in each sample were determined following Hein and Longstaffe (1983). Background-subtracted peak-heights were measured for glycol-solvated powders laid down on ceramic tiles and the following form-factors applied to clay peak heights: smectitic clay (001), x1; illitic clay (001), x4; kaolinitic clay (001), x 2 (as used by Hein and Longstaffe,

1983). To account for the small amounts of quartz present, the background-subtracted peak height of its (100) diffraction (4.26Å, 0.426 nm) was also measured, to which a form factor of x3 was applied. Quartz's 4.26Å, rather than the 3.343 Å diffraction was used to avoid interferences from the illite (003). Experimental calibration of quartz-kaolinite mixtures suggests that this approach will yield a reasonable estimate of quartz content for abundances generally lower than ~15%, though the bias is to overestimate quartz.

Mixed-layered clays were identified in air-dried (~50% RH), preferred-oriented samples, based on the presence of a broad diffraction peak typically ranging from 14.4 to 15.2 Å that is associated with a high background at low angles from the diffraction (Fig. DR3), and a pronounced shoulder at the high angle side of the diffraction straying towards the 12.5 to 13 Å position. Upon treatment with ethylene glycol, samples containing both smectite and mixed-layer illite-smecite clays typically then exhibit a diffraction doublet, with one peak at ~16.8 to 17.0 Å and the second peak, typically climbing the high angle side of the first peak, having a position at ~14.6 to 16.0 Å (commonly ~14.7 Å, see Figure DR3A). Upon heating to 550°C, both of these peaks disappeared and were replaced by a strong diffraction at ~10 Å. That chlorite layers, or even vermiculite layers form part of the mixed-layer phase cannot be ruled out based on the existing XRD data. The (060) diffraction data for these swelling clays suggest that they are dioctahedral. Typical examples of diffractograms of samples containing illite-smectite (Fig. DR3A) and no illite-smectite (Fig. DR3B) are included for reference.

The K/S ratio calculation was done using the (001) background-subtracted peak heights from the glycol-solvated samples after these heights had been adjusted using the form-factors described above.

Physical separation of the different clay species proved impossible, in part because of the limited sample volume available from the existing cores. Instead, the bulk <2 μm size-fraction was analyzed for oxygen stable isotopes ($\delta^{18}O_{Clays}$). The $\delta^{18}O_{Clays}$ values, reported relative to Vienna Standard Mean Ocean Water (VSMOW), were measured at the University of Western Ontario, in dual-inlet mode, using a Thermo Finnigan Delta XL mass spectrometer. Approximately 9 mg of sample powder were placed into spring-loaded sample holders, evacuated overnight at ~150ºC, and then loaded into nickel reaction vessels and evacuated for another 3 hours at 150ºC. The sample powders were then reacted overnight at ~580ºC with ClF_3 to release the silicate-bound oxygen (see Clayton and Mayeda, 1963; Borthwick and Harmon, 1982), which was then converted to CO_2 for isotopic measurement. Precision based on replicate samples was better than 0.2‰.

ASSESSING THE IMPACT OF CLAY MIXING OVER $\delta^{18}O_{Clays}$

To assess whether the observed trend in $\delta^{18}O_{Clays}$ values could result from a shift in the assemblage of clay minerals presents, we first assumed that kaolinite and smectite each had constant (but distinct) isotopic compositions, and derived a best fit (quadratic) regression between the $\delta^{18}O_{Clays}$ values and kaolinite fraction ($F_{Kaolinite}$, from 0-100 %; Fig. DR1, $r^2 = 0.88$):

$$\delta^{18}O_{Clays} = 23.0 + 0.005 * F_{Kaolinite} - 0.02 * F_{Kaolinite}{}^{2} \quad (1)$$

Based on equation (1) we can express $\delta^{18}O_{smectite}$ values for samples containing no kaolinite as:

$$\delta^{18}O_{Smectite} = \frac{23.0 - F_{Illite} * \delta^{18}O_{Illite} - F_{Quartz} * \delta^{18}O_{Quartz}}{F_{Smectite}} \quad (2)$$

where $F_{Smectite}$, F_{Illite} and F_{Quartz} are the respective percentages of each phase in the <2 μm size-fraction. The above equation can be simplified by assuming that neither the proportion of illite and quartz in the clay fraction nor their isotopic compositions vary significantly through the section. The validity of these assumptions is supported by the following observations: (1) the abundance of both illite and quartz is relatively constant throughout the section, and (2) no significant correlation exists between the abundance of either quartz or illite and the $\delta^{18}O_{Clays}$ values (Fig. DR1). We can thus define a constant *k* as:

$$k = F_{Illite} * \delta^{18}O_{Illite} + F_{Quartz} * \delta^{18}O_{Quartz} \quad (3)$$

Because $F_{Illite} + F_{Quartz}$ is constant (0.44 in average), $F_{Kaolinite} + F_{Smectite} = 0.56$, and for the case considered $F_{Kaolinite} = 0$, we can rewrite equation (2) as:

$$\delta^{18}O_{Smectite} = \frac{23.0 - k}{F_{Smectite}} = \frac{23.0 - k}{0.56} \quad (4)$$

We can express $\delta^{18}O_{Kaolinite}$ following similar steps as in equations (1-4) by using the intersect at $F_{Smectite} = 0$ of the best fit (quadratic) correlation (R^2 of 0.96) of $\delta^{18}O_{Clays}$ versus $F_{Smectite}$ (Fig. DR1):

$$\delta^{18}O_{Kaolinite} = \frac{17.5 - k}{0.56} \quad (5)$$

Although we cannot directly calculate $\delta^{18}O_{smectite}$ or $\delta^{18}O_{kaolinite}$, we can estimate the isotopic difference between the two minerals:

$$\delta^{18}O_{Smectite} - \delta^{18}O_{Kaolinite} = \frac{23.0 - 17.5}{0.56} \cong 10‰ \quad (6)$$

These results suggest that the shape of the measured $\delta^{18}O_{Clays}$ curve (Fig. 2) could be obtained by simple mixing between a smectitic phase and a kaolinitic phase as long as the offset in $\delta^{18}O$ values between the two minerals is ~ 10‰. This isotopic separation is much larger than expected (≤0.5 ‰) for kaolinite and smectite formed during weathering at similar temperatures from water of similar oxygen isotopic compositions.

Assuming a constant 10‰ offset between the isotopic composition of smectite and kaolinite, we can calculate the difference in $\delta^{18}O_{clays}$ between a reference sample (REF) and any other given sample ($\Delta\delta^{18}O_{clays[REF-Sample]}$). We can simplify the estimate by using only the measured kaolinite content of the samples and the isotopic difference between kaolinite and smectite because we know that $F_{smectite}$=0.56-$F_{kaolinite}$, and $\delta^{18}O_{smectite} = \delta^{18}O_{kaolinite}$+10‰. Hence, the Δ between two samples can be written as:

$$\Delta\delta^{18}O_{clays[REF-Sample]} = (F_{kaolinite[REF]} - F_{kaolinite[Sample]}) * 10‰ \quad (7)$$

A synthetic $\delta^{18}O_{clays}$ curve can be created by choosing a reference point on the measured curve, and the error for each calculated point on the curve is ±0.8‰ (Fig.DR2, error is linked to measurement errors in $\delta^{18}O_{clays}$ and XRD values for kaolinite). We have selected a reference point that best anchors the calculated curve on the measured curve (REF= sample at 357.67 mbs with a $\delta^{18}O_{clays}$ = 21.1‰ and $F_{kaolinite}$= 0.3548).

REFERENCES

Borthwick, J., and Harmon, R. S., 1982, A note regarding ClF_3 as an alternative to BrF_5 for oxygen isotope analysis: Geochimica et Cosmochimica Acta, v. 46, no. 9, p. 1665-1668.

Brindley, G. W., and Brown, G., 1980, Crystal structures of clay minerals and their X-ray identification, Monograph - Mineralogical Society, v. 5.

Clayton, R. N., and Mayeda, T. K., 1963, The use of bromine pentafluoride in the extraction of oxygen from oxides and silicates for isotopic analysis: Geochimica et Cosmochimica Acta, v. 27, no. 1, p. 43-52.

Gibson, T. G., Bybell, L. M., and Mason, D. B., 2000, Stratigraphic and climatic implications of clay mineral changes around the Paleocene/Eocene boundary of the northeastern US margin: Sedimentary Geology, v. 134, p. 65-92.

Hein, F. J., and Longstaffe, F. J., 1983, Geotechnical, sedimentological and mineralogical investigations in arctic fjords, *in* Syvitski, J. P. M., and Blakeney, C. P., eds., Sedimentology of Arctic Fjords Experiment: HU 82-031 Data Report, Vol. 1, Volume 12, p. 11-11 to 11-158.

John, C. M., Bohaty, S. M., Zachos, J. C., Gibbs, S., Brinkhuis, H., Sluijs, A., and Bralower, T., 2008, Impact of the Paleocene-Eocene thermal maximum on continental margins and implications for the carbon cycle in near-shore environments: Paleoceanography, v. 23, p. PA2217.

Miller, K. G., Sugarman, P. J., Browning, J. V., Kominz, M. A., Olsson, R. K., Feigenson, M. D., and Hernandez, J. C., 2004, Upper Cretaceous sequences and sea-level history, New Jersey coastal plain.: GSA Bulletin, v. 116, no. 3-4, p. 368-393.

Miller, K. G., Sugarman, P. J., Browning, J. V., Olsson, R. K., Pekar, S. F., Reilly, T. J., Cramer, B. S., Aubry, M.-P., Lawrence, R. P., Curran, J., Stewart, M., Metzger, J. M., Uptegrove, J., Bukry, D., Burckle, L. H., Wright, J. D., Feigenson, M. D., Brenner, G. J., and Dalton, R. F., 1998, Initial Reports, Leg 174AX, College Station, TX, Proceedings of the Ocean Drilling Program.

Moore, D. M., and Reynolds, R. C., 1997, X-ray diffraction and the identification and analysis of clay minerals, Oxford, Oxford University Press, 378 p.

Sluijs, A., Brinkhuis, H., Schouten, S., Bohaty, S., John, C. M., Zachos, J. C., Reichart, G.-J., Sinninghe Damsté, J., Crouch, E., and Dickens, G. R., 2007, Environmental change before the rapid carbon injection at the Palaeocene/Eocene boundary: Nature, v. 450, no. 7173, p. 1218-1221.

REPOSITORY FIGURE CAPTIONS

Figure DR1: Location of the Bass River drill site (red star) on the New Jersey coastal plains. The insert shows the position of New Jersey on a paleogeographic map of the Eocene.

Figure DR2: Oxygen isotope compositions of the <2 μm size-fraction ($\delta^{18}O_{Clays}$) versus A: Percentage of quartz (F_{Quartz}, green data points) and percentage of illite (F_{Illite}, red data points) in the <2μm fraction; B: Percentage of kaolinite ($F_{Kaolinite}$) in the <2μm fraction, and C: Percentage of smectite ($F_{Smectite}$) in the <2μm fraction. F_{Quartz} and F_{Illite} are relatively constant, and show no significant correlations with $\delta^{18}O_{Clays}$ values. $F_{Kaolinite}$ and $F_{Smectite}$ (panels B and C) show a strong correlation with $\delta^{18}O_{Clays}$ values suggesting that mixing between these two phases controls the variation in oxygen isotopic composition of the <2 μm size-fraction.

Figure DR3 : Typical diffractograms of samples A) containing illite-smectite and B) without illite smectite. Vertical axis are intensity in counts per seconds for the air-dried (red diffractogram and red axis values) and the ethylen-glycol solvated run (blue line, blue axis values). Horizontal axis are diffraction angle (2θ). Identified minerals: S = smectite; I/S = mixed-layer clay (probably illite-smectite but I can't be sure from these data), K = kaolinite, I = illite, and Q = quartz.

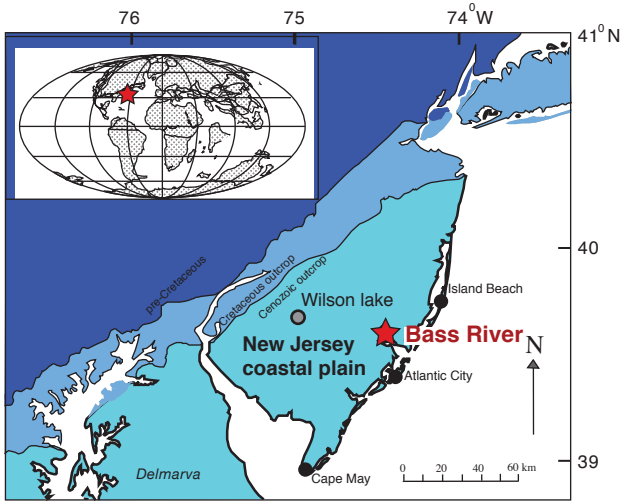
76
75
74°W
41°N
40
39
pre-Cretaceous
Cretaceous outcrop
Cenozoic outcrop
Wilson lake
Island Beach
Bass River
New Jersey
coastal plain
Atlantic City
N
Delmarva
Cape May
0 20 40 60 km

Figure DR1

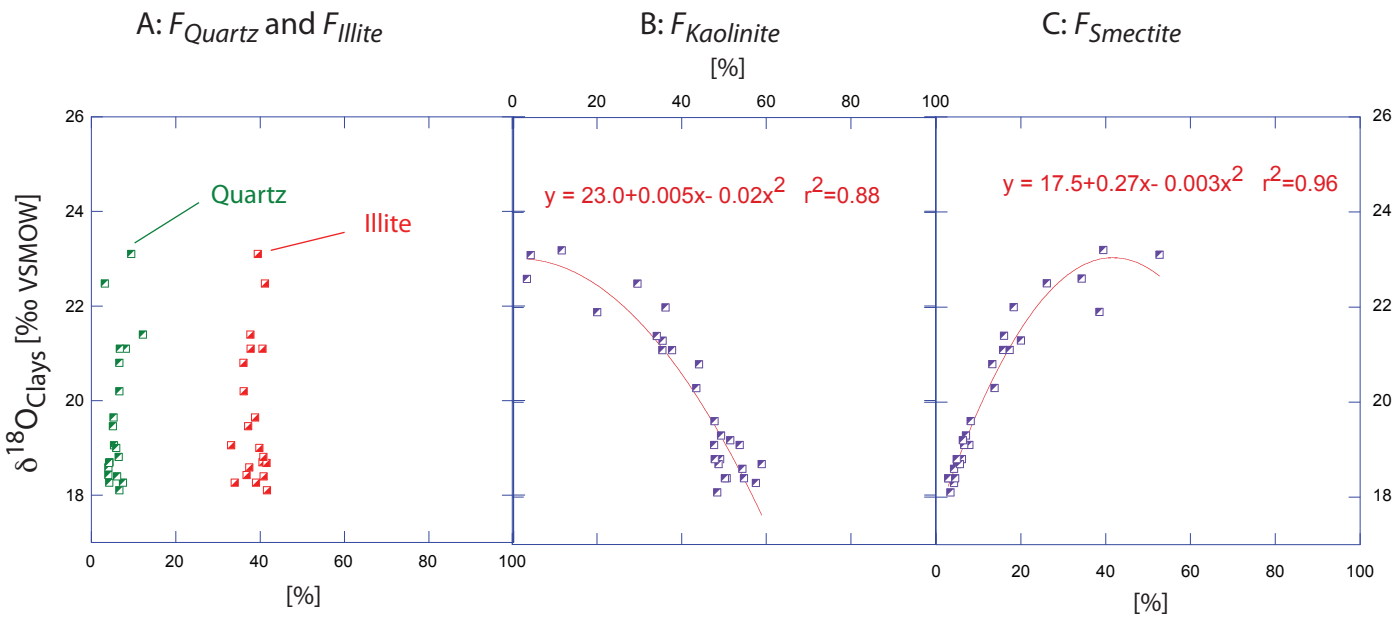
A: F_{Quartz} and F_{Illite}
B: $F_{Kaolinite}$
C: $F_{Smectite}$
$\delta^{18}O_{Clays}$ [‰ VSMOW]
Quartz
Illite
y = 23.0+0.005x- 0.02x^2 r^2=0.88
y = 17.5+0.27x- 0.003x^2 r^2=0.96
[%]
[%]
[%]

Figure DR2

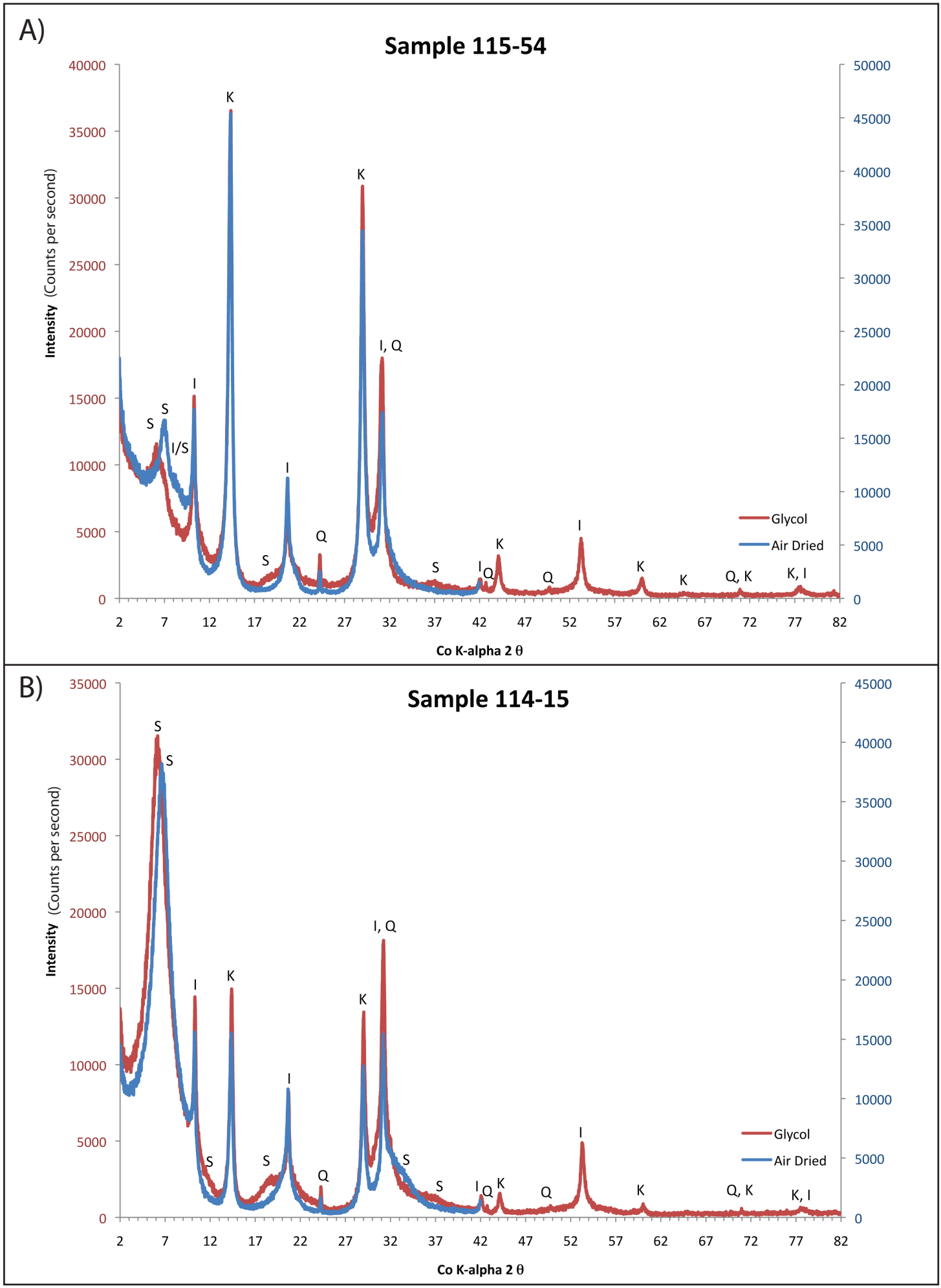
A)
Sample 115-54
Intensity (Counts per second)
Co K-alpha 2 θ
Glycol
Air Dried
B)
Sample 114-15
Intensity (Counts per second)
Co K-alpha 2 θ
Glycol
Air Dried

Figure DR3